Contemporary Mathematics
https://ojs.wiserpub.com/index.php/CM/

Research Article

Solving Fractional Nonlinear Harry-Dym and Rosenau-Hyman Equations Using the Conformable Fractional Derivative

Naveed Iqbal[1*], **Meshari Alesemi**[2]

[1]Department of Mathematics, College of Science, University of Ha'il, Ha'il, 2440, Saudi Arabia
[2]Department of Mathematics, College of Science, University of Bisha, P.O. Box 511, Bisha, 61922, Saudi Arabia
E-mail: n.iqbal@uoh.edu.sa

Received: 5 June 2025; **Revised:** 28 June 2025; **Accepted:** 1 July 2025

Abstract: The paper discusses the application of the Residual Power Series Conformable Method (RPSCM) and a new iteration method to solve the fractional nonlinear Harry-Dym and Rosenau-Hyman to employ conformable fractional derivatives. The suggested techniques focus on the non-linearity and high dimensionality of these equations and would provide sufficiently accurate and efficient approximate solutions. The RPSCM combines a power series expansion and residual error correction, whereas the iterative method enhances convergence by employing a distinct approach. The graphical and numerical performances of the two methods are compelling, as the figures represent the simulated solution behaviors and the sensitive changes resulting from variations in the fractional order. The superior precision of the techniques is also evident when the results obtained by the methods are compared with standards presented in tables in solving nonlinear fractional problems across various applied fields.

***Keywords*:** residual power series conformable method, new iterative method, the fractional nonlinear Harry-Dym equation and Rosenau-Hyman equations, conformable fractional derivative

MSC: 35A35, 26A33, 35A22

1. Introduction

Fractional calculus is the study of integrals and classical derivatives extended or generalized to non-integer order instances, and it has received a great deal of scholarly interest in the past several decades. In the study of Fractional derivatives can be found in a variety of technical and physical systems, including viscoelasticity, groundwater, the propagation of waves, finances, and fluid mechanics [1, 2]. Several researchers have examined theoretical outcomes derived from the the presence of fractional differential equation solutions and their uniqueness in different formats; some examples of these investigations are [3–7]. Many fractional differential problems are clearly either without closed form solutions or have too complex an analytical solution to be of much use. Because of this, numerous authors have developed a variety of numerical approximation techniques. These include the He's variational iteration method, Fourier spectral methods, Finite difference schemes, the homotopy analysis approach, Adomian's decomposition, and many more that are categorized in [2]. For comprehensive research on the solution of fractional differential equations, we direct our readers to the classic books and papers [1, 2].

DOI: https://doi.org/10.37256/cm.6420257382

We examine fractional Harry Dym equation and fractional Rosenau-Hyman equation both have the following forms:

$$\frac{\partial \upsilon}{\partial \rho} - \upsilon^3(\vartheta,\, \rho)\frac{\partial^3 \upsilon(\vartheta,\, \rho)}{\partial \vartheta^3} = 0 \tag{1}$$

using the initial condition's

$$\upsilon(\vartheta,\, 0) = \left(a - \frac{3\sqrt{b}\vartheta}{2}\right)^{2/3}. \tag{2}$$

and

$$\frac{\partial \upsilon}{\partial \rho} - \upsilon(\vartheta,\, \rho)\frac{\partial^3 \upsilon(\vartheta,\, \rho)}{\partial \vartheta^3} - \upsilon(\vartheta,\, \rho)\frac{\partial \upsilon(\vartheta,\, \rho)}{\partial \vartheta} - 3\frac{\partial \upsilon(\vartheta,\, \rho)}{\partial \vartheta}\frac{\partial^2 \upsilon(\vartheta,\, \rho)}{\partial \vartheta^2} = 0. \tag{3}$$

using the initial condition's

$$\upsilon(\vartheta,\, 0) = -\frac{8}{3}c\cos^2\left(\frac{\vartheta}{4}\right). \tag{4}$$

A vital dynamical equation utilized in many different physical systems is the Harry Dym. Harry Dym is credited with developing the Harry Dym equation in an unpublished 1973-1974 study, which was first published in Kruskal and Moser [8]. It represents a system where nonlinearity and dispersion are closely related. Despite not having the Painleve property, Harry Dymis' completely integrable nonlinear evolution equation complies with an endless number of conversion rules. The Korteweg-de Vries equation, which has been used to hydrodynamic issues, is closely connected to the Harry Dym equation [9]. The Harry Dym equation's Lax pair is connected to the Sturm-Liouville operator. The Liouville transformation spectrally converts this operator into the Schrodinger operator [10]. The Rosenau-Hyman equation was discovered by Rosenau and Hyman [11] and occurs when compaction solutions cause patterns to form in liquid drops. In mathematical physics and applied sciences, the Rosenau-Hyman equation compact on research is helpful [12–15].

Considering the Residual Power Series Conformable Method (RPSCM), the objective of the given study is the development and implementation of the effective analytical method applicable to solving the problem of the nonlinear conformable time-fractional motion of gases, both in the homogeneous case and in the inhomogeneous one. This means that the Conditional Random Sampling Method (CRSM) can be an effective analytic tool to determine power series solution of a number of systems of ordinary differential equations, partial differential equations, integral equations and fractional fuzzy operators, and integro-differentials [16–20]. It is a high level approximation technique that can be applied directly and one which is flexible enough to provide exact solution to linear and nonlinear cases without any need of any linearization, substitution or constraints of the nature of the physical system. The CRSM approach does not require a comparison of the relevant coefficients and does not require a connection of a recursion one as it is in the traditional PS method. The correlation between the residual error and the index of residual error and required conformable fractional derivatives is also calculated in case of finding series coefficients which yields a system of algebraic equations having one variable or more variables. In some situations, especially where the analytic solutions are polynomial, CRSM gives a closed representation of a series solution.

Jafari and Daftardar-Gejji [21] provided the Novel Iterative Technique (NIM) in 2006, and It is now an effective mathematical approach to evaluating functional equations, both non-linear and linear. Numerous nonlinear problems, such as algebraic equations, integral equations, and partial or ordinary differential equations of both fractional and integer order, have been solved using NIM. The unique features of NIM include its ease of use and comprehension, which make it available to a broad range of scholars and practitioners. Compared to established techniques such as the homotopy perturbation method [22], the ADM [23], and the VIM [24], NIM has shown improved performance and better efficiency.That's why people dealing with complex nonlinear situations find it popular [25].

2. Preliminaries

The most often used definitions of fractional derivatives of order $\sigma > 0$ are the Riemann-Liouville and Caputo fractional derivatives.

Definition 1 The fractional Riemann-Liouville derivative operator $D^{\sigma}\omega(\vartheta)$ defined as [26]:

$$D^{\sigma}\omega(\vartheta) = \frac{d^{q}}{d\vartheta^{q}}\left[\frac{1}{\Gamma(q-\sigma)}\int_{\sigma}^{\vartheta}\frac{\omega(\rho)}{(\vartheta-\rho)^{\sigma+1-q}}d\rho\right] \tag{5}$$

in which $q-1 < \sigma < q$ and $\sigma > 0$.

Definition 2 The fractional Caputo derivative of order σ defined as [27]:

$$D_{*}^{\sigma}\omega(\vartheta) = J^{\eta-\sigma}D^{\sigma}\omega(\vartheta) = \frac{1}{\Gamma(\eta-\sigma)}\int_{\sigma}^{\vartheta}(\vartheta-\rho)^{\eta-\sigma-1}\left(\frac{d}{d\rho}\right)^{\eta}\omega(\rho)d\rho \tag{6}$$

where the fractional derivative of the Caputo operator is indicated by $\sigma > 0$ for $\eta \in \mathbb{N}$, $\eta - 1 < \sigma < \eta$, $D_{*}^{\sigma}(.)$ and $J^{\eta-\sigma}(.)$ indicates Caputo fractional integral operator. A new definition known as the "conformable fractional derivative" was recently put out by Khalil et al. [28].

Definition 3 The definition of the "conformable fractional derivative" of a function of σ-th order is

$$T_{\sigma}(\omega)(\rho) = \lim_{\varepsilon\to 0}\frac{\omega\left(\rho+\varepsilon\rho^{1-\sigma}\right)-(\omega)(\rho)}{\varepsilon} \tag{7}$$

for every $\rho > 0,\ \sigma \in (0,\ 1)$ and for $f : [0,\ \infty) \to R$.

The following theorem [27] lists the characteristics of this new definition.

Definition 4 For a function with n variables $\vartheta_1,\ \ldots,\ \vartheta_b$, ω represents the conformable partial derivatives of ω of order $a \in (0,\ 1)$. The following is the definition of in ϑ_i [29].

$$\frac{d^{\sigma}}{d\vartheta_i^{\sigma}}\omega(\vartheta_1,\ \ldots,\ \vartheta_\eta) = \lim_{\varepsilon\to 0}\frac{\omega\left(\vartheta_1,\ \ldots,\ \vartheta_{i-1},\ \vartheta_i+\varepsilon\vartheta_i^{1-\sigma},\ \ldots,\ \vartheta_\eta\right)-\omega(\vartheta_1,\ \ldots,\ \vartheta_\eta)}{\varepsilon} \tag{8}$$

Definition 5 The definition of the conformable integral of a function ω beginning from $a \geq 0$ is [30].

$$I_{\sigma}^{a}(\omega)(s) = \int_{a}^{s}\frac{\omega(\rho)}{\rho^{1-\sigma}}d\rho \tag{9}$$

3. Residual power series conformable method

Some important definitions and theorems pertaining to residual power series will be presented in this section.

Theorem 1 For some $0 < \sigma \leq 1$, the fractional power series expansion of ω takes the following form if ρ_0 is an indefinitely σ-differentiable function at a neighborhood of a point ρ_0.

$$\omega(\rho) = \sum_{k=0}^{\infty} \frac{\left(T_\sigma^{\rho_0}\omega\right)^{(k)}(\rho_0)(\rho-\rho_0)^{k\vartheta}}{\sigma^k k!}, \quad \rho_0 < \rho < \rho_0 + R^{\frac{1}{\vartheta}}, \quad R > 0 \tag{10}$$

In this case $(T_\sigma * \omega)^{(k)}(\rho_0)^{\rho_0}$ is used to denote the fractional derivative k-times [31].

Definition 6 A series of fractional powers pertaining to $\rho_0 = 0$ is defined as $\sum_{\eta=0}^{\infty} \omega_\eta(\vartheta)\rho^{\eta\vartheta}$ for $0 \leq m-1 < \sigma < m$, while ρ is a variable and $\omega_\eta(\vartheta)$ generally functions that are referred to as the values of the series [32].

Theorem 2 Assuming that $\upsilon(\vartheta,\ \rho)$ at $\rho_0 = 0$ is represented by a multiple fractional power series is expressed as:

$$\upsilon(\vartheta,\ \rho) = \sum_{\vartheta=0}^{\infty} \omega_\vartheta(\vartheta)\rho^{va},\ 0 \leq m-1 < \sigma < m, \quad \vartheta \in I, \quad 0 \leq \rho \leq R^\rho \tag{11}$$

Then $\omega_n(x) = \dfrac{u_{i(a\vartheta)}^{(\vartheta,\ 0)}}{a_{n1}^4}$ if $n = 0,\ 1,\ 2\ldots$ are continuots on $I \times \left(0,\ R^{\frac{1}{2}}\right)$ and $u_z^{(ma)}(\vartheta,\ \rho)$. Let's examine a nonlinear fractional differential equation of the following kind to demonstrate the core concept of RPSCM:

$$T_\vartheta \upsilon(\vartheta,\ \rho) + N[\vartheta]\upsilon(\vartheta,\ \rho) + R[\vartheta]\upsilon(\vartheta,\ \rho) = c(\vartheta,\ \rho), \quad \vartheta \in \mathbf{R}, \quad \eta - 1 < \eta\vartheta \leq \eta, \quad \rho > 0, \tag{12}$$

given with the initial condition

$$\omega_0(\vartheta) = \upsilon(\vartheta,\ 0) = \omega(\vartheta) \tag{13}$$

In this instance, $R[\vartheta]$ is linear, and $N[\vartheta]\ c(\vartheta,\ \rho)$ is a continuous function, and is a non-linear operator. The fractional power series expansion around $\rho = 0$ is expressed using the RPSCM technique as the solution of Equation (11) subject to (12).

$$\omega_{(\eta-1)}(\vartheta) = T_i^{(\eta-1)\vartheta}\upsilon(\vartheta,\ 0) = h(\vartheta) \tag{14}$$

The solution's expansion form is provided by

$$\upsilon(\vartheta,\ \rho) = \omega(\vartheta) + \sum_{\eta=1}^{\infty} \omega_\eta(\vartheta)\frac{\rho^{\eta\vartheta}}{a^\eta \eta!} \tag{15}$$

We may write $w_k(\vartheta,\ \rho)$, the k, by taking the next step. $\upsilon(\vartheta,\ \rho)$ truncated series, as follows:

$$\upsilon_k(\vartheta,\ \rho) = \omega(\vartheta) + \sum_{\eta=1}^{k} \omega_s(\vartheta)\frac{\rho^{\eta}\sigma}{a^{\eta}\eta!} \tag{16}$$

If $\upsilon_1(\vartheta,\ \rho)$, the 1. Residual Power Series Method (RPSM) approximation solution is

$$\upsilon_1(\vartheta,\ \rho) = \omega(\vartheta) + \omega_1(\vartheta)\frac{\rho^{\vartheta}}{\vartheta^{\eta}} \tag{17}$$

Consequently, $\upsilon_k(\vartheta,\ \rho)$ might be rewritten as

$$\upsilon_k(\vartheta,\ \omega) = \omega(\vartheta) + \omega_1(\vartheta)\frac{\rho^{z}}{\sigma^{\eta}} + \sum_{\eta=2}^{k} \omega_s(\vartheta)\frac{\rho^{k\sigma}}{\sigma^{\eta}\eta!} \tag{18}$$

for $0 < \sigma \leq 1,\ 0 \leq \rho < \mathbb{R}^{\frac{1}{v}},\ \vartheta \in I$ and $k = 2,\ 3,\ 4,\ \ldots$.

Initially, we represent the residual function as

$$Re\vartheta(\vartheta,\ \rho) = T_a\upsilon(\vartheta,\ \rho) + N[\vartheta]\upsilon(\vartheta,\ \rho) + R[\vartheta]\upsilon(\vartheta,\ \rho) - c(\vartheta,\ \rho) \tag{19}$$

With the residual function k as

$$\mathrm{Rers}(\vartheta,\ \rho) = T_a\upsilon_k(\vartheta,\ \rho) + N[\vartheta]\upsilon_k(\vartheta,\ \rho) + R[\vartheta]\upsilon_k(\vartheta,\ \rho) - g(\vartheta,\ \rho),\ k = 1,\ 2,\ 3,\ \ldots \tag{20}$$

Clearly, $\mathrm{Res}(\vartheta,\ \rho) = 0$ as well as $\lim_{k\to\infty}\mathrm{Res}_k(\vartheta,\ \rho) = \mathrm{Res}(\vartheta,\ \rho)$ for every $\vartheta \in I$ and $0 \leq \rho$. As a result, $\frac{\partial^{(\eta-1)}\sigma}{\partial\rho^{(\eta-1)\sigma}}\mathrm{Res}_k(\vartheta,\ \rho)$ was actually produced for $\ldots,\ k,\ \eta = 1,\ 2,\ 3,$ since in the sense of conformable, a constant's fractional derivative is zero [33–35]. To solve the equation $\frac{\partial^{\eta-1)\sigma}}{\partial\rho^{(n-1)\sigma}}\mathrm{Res}_k(\vartheta,\ 0) = 0$ provides the expected $\omega_\eta(\vartheta)$ coefficients. Consequently, the approximate solutions $\upsilon_\eta(\vartheta,\ \rho)$ can be derived, accordingly.

The following theorem regarding the method's convergence analysis can be expressed.

Theorem 3 If $0 < K < 1$ and $0 < \rho < R < 1$, then $\left\|\upsilon_{\eta+1}(\vartheta,\ \rho)\right\| \leq K\left\|\upsilon_\eta(\vartheta,\ \rho)\right\|$ for all $\eta \in \mathbb{N}$, therefore a precise solution converges to the sequence of approximate solutions [36].

Proof. For every $0 < \rho < R < 1$, we possess

$$\left\|\upsilon(\vartheta,\ \rho) - \upsilon_\eta(\vartheta,\ \rho)\right\| = \left\|\sum_{\iota=\eta+1}^{\infty}\upsilon_\iota(\vartheta,\ \rho)\right\| \leq \sum_{\iota=\eta+1}^{\infty}\left\|\upsilon_\iota(\vartheta,\ \rho)\right\| \leq \left\|\omega(\vartheta)\right\|\sum_{\iota=\eta+1}^{\infty}K^{\iota} = \frac{K^{\eta+1}}{1-K}\left\|\omega(\vartheta)\right\|^{\eta\to\infty}0. \tag{21}$$

4. New iterative method

For the purpose of solving the functional equation, Daftardar-Gejji and Jafari [21] have presented a novel iterative technique.

$$\upsilon(\bar{\vartheta},\, \rho) = p(\bar{\vartheta},\, \rho) + L(\upsilon(\bar{\vartheta},\, \rho)) + N(\upsilon(\bar{\vartheta},\, \rho)), \tag{22}$$

where ω is a specified function, and linear and non-linear functions of υ are given by L and N, respectively, $\bar{\vartheta} = (\vartheta_1,\, \vartheta_2,\, \cdots,\, \vartheta_\eta)$. We are trying to find a solution υ of (7) that has the following series form:

$$\upsilon(\bar{\vartheta},\, \rho) = \sum_{\iota=0}^{\infty} \upsilon_\iota(\bar{\vartheta},\, \rho) \tag{23}$$

L is linear, so

$$L\left(\sum_{\iota=0}^{\infty} \upsilon_\iota\right) = \sum_{\iota=0}^{\infty} L(\upsilon_\iota). \tag{24}$$

As can be seen in [21], the nonlinear operator N is broken down as

$$N\left(\sum_{\iota=0}^{\infty} \upsilon_\iota\right) = N(\upsilon_0) + \sum_{\iota=1}^{\infty} \left\{ N\left(\sum_{j=0}^{\iota} \upsilon_j\right) - N\left(\sum_{j=0}^{\iota-1} \upsilon_j\right) \right\}. \tag{25}$$

Equations (8)-(10) show that (7) is equal to

$$\sum_{\iota=1}^{\infty} \upsilon_\iota = \omega + \sum_{\iota=0}^{\infty} L(\upsilon_\iota) + N(\upsilon_0) + \sum_{\iota=1}^{\infty} \left\{ N\left(\sum_{j=0}^{\iota} \upsilon_j\right) - N\left(\sum_{j=0}^{\iota-1} \upsilon_j\right) \right\} \tag{26}$$

The recurrence relation is defined as:

$$\begin{aligned} &\upsilon_0 = \omega \\ &\upsilon_1 = L(\upsilon_0) + N(\upsilon_0) \\ &\upsilon_{m+1} = L(\upsilon_m) + N(\upsilon_0 + \cdots + \upsilon_m) - N(\upsilon_0 + \cdots + \upsilon_{m-1}),\ m = 1,\, 2,\, \cdots \end{aligned} \tag{27}$$

Then,

$$(\upsilon_1 + \cdots + \upsilon_{m+1}) = L(\upsilon_0 + \cdots + \upsilon_m) + N(\upsilon_0 + \cdots + \upsilon_m),\ m = 1,\, 2,\, \cdots, \tag{28}$$

and

$$\sum_{\iota=0}^{\infty} \upsilon_{\iota} = \omega + L\left(\sum_{\iota=0}^{\infty} \upsilon_{\iota}\right) + N\left(\sum_{\iota=0}^{\infty} \upsilon_{\iota}\right). \tag{29}$$

The approximate solution for the k-term of Equations (7)-(8) is $\upsilon = \upsilon_0 + \upsilon_1 + \cdots + \upsilon_{k-1}$. We direct the reader to paper [21] for the method's convergence.

5. Applications of residual power series conformable method

5.1 *Problem 1*

Let the fractional nonlinear Harry Dym Equation:

$$\frac{\partial \upsilon}{\partial \rho} - \upsilon^3(\vartheta,\, \rho)\frac{\partial^3 \upsilon(\vartheta,\, \rho)}{\partial \vartheta^3} = 0 \tag{30}$$

using the initial condition's

$$\upsilon(\vartheta,\, 0) = \omega(\vartheta) = \left(a - \frac{3\sqrt{b}\vartheta}{2}\right)^{2/3}. \tag{31}$$

The exact solution is found for the related integer order problem $a = 1$ and $b = 1$ in the limit sense as,

$$\upsilon(\vartheta,\, \rho) = \left(a - \frac{3}{2}\sqrt{b}(\vartheta + bt)\right)^{2/3}. \tag{32}$$

For residual power series, where $\upsilon = \upsilon(\vartheta,\, \rho)$.

$$\upsilon(\vartheta,\, \rho) = \omega(\vartheta) + \sum_{\eta=1}^{\infty} \omega_{\eta}(\vartheta)\frac{\rho^{\eta\vartheta}}{\sigma^{\eta}\eta!} \tag{33}$$

and the truncated k-th series of $\upsilon[\vartheta,\, \rho]$.

$$\upsilon_k(\vartheta,\, \rho) = \omega(\vartheta) + \sum_{\eta=1}^{k} \omega_{\eta}(\vartheta)\frac{\rho^{\eta}}{a^{\eta}\eta!}, \quad k = 1,\, 2,\, 3,\, \ldots \tag{34}$$

A residual function of k-th of nonlinear Harry Dym equation:

$$\mathrm{Rer}\, \upsilon_k(\vartheta,\, \rho) = \frac{\partial \upsilon_k}{\partial \rho} - \upsilon_k^3(\vartheta,\, \rho)\frac{\partial^3 \upsilon_k(\vartheta,\, \rho)}{\partial \vartheta^3}. \tag{35}$$

The 1st truncated series $\upsilon_1(\vartheta,\ \rho) = \omega(\vartheta) + \omega_1(\vartheta)\dfrac{\rho^\sigma}{\sigma}$ should be substituted into the $1s\rho$ truncated residual function in order to get the coefficients $\omega_1(\vartheta)$ in $\upsilon_1(\vartheta,\ \rho)$.

$$\mathrm{Res}\upsilon_1(\vartheta,\ \rho) = \omega_1(\vartheta) - \left(\omega(\vartheta) + \frac{\rho^a \omega_1(\vartheta)}{\sigma}\right)^3 \left(\omega'''(\vartheta) + \frac{\rho^a \omega_1'''(\vartheta)}{\sigma}\right). \tag{36}$$

Using equation $\mathrm{Res}\upsilon_1(\vartheta,\ \rho)$, we can now substitute $\rho = 0$ and get

$$\mathrm{Resm}\upsilon_1(\vartheta,\ 0) = \omega_1(\vartheta) - \omega_0^3(\vartheta)\omega_0'''(\vartheta). \tag{37}$$

Thus for $\mathrm{Re}\upsilon_1(\vartheta,\ 0) = 0$

$$\omega_1(\vartheta) = \omega_0^3(\vartheta)\omega_0'''(\vartheta). \tag{38}$$

$$\omega_1(\vartheta) = -\frac{b^{3/2}}{\sqrt[3]{a - \dfrac{3\sqrt{b}\vartheta}{2}}}. \tag{39}$$

Consequently, the first RPS approximations of the nonlinear Harry Dym:

$$\upsilon_1(\vartheta,\ \rho) = \omega(\vartheta) + \frac{\rho^\sigma(\omega_0^3(\vartheta)\omega_0'''(\vartheta))}{\sigma}. \tag{40}$$

$$\upsilon_1(\vartheta,\ \rho) = \left(a - \frac{3\sqrt{b}\vartheta}{2}\right)^{2/3} + \frac{\left(-\dfrac{b^{3/2}}{3\sqrt{a - \dfrac{3\sqrt{b}\vartheta}{2}}}\right)\rho^\sigma}{\sigma}. \tag{41}$$

Once more, we use the second truncated series solution $\upsilon_2(\vartheta,\ \rho) = \omega(\vartheta) + \omega_1(\vartheta)\dfrac{\rho^\sigma}{\sigma} + \omega_2(\vartheta)\dfrac{\rho^{2\sigma}}{2\sigma^2}$ to find the second unknown coefficient $\omega_2(\vartheta)$.

$$\begin{aligned}\mathrm{Res}\upsilon_2(\vartheta,\ \rho) &= \omega_1(\vartheta) \\ &+ \frac{\rho^\sigma \omega_2(\vartheta)}{\sigma} \\ &- \left(\omega(\vartheta) + \frac{\rho^\sigma \omega_1(\vartheta)}{\sigma} + \frac{\rho^{2\sigma}\omega_2(\vartheta)}{2\sigma^2}\right)^3 \left(\omega'''(\vartheta) + \frac{\rho^\sigma \omega_1'''(\vartheta)}{\sigma} + \frac{\rho^{2\sigma}\omega_1'''(\vartheta)}{2\sigma^2}\right)\end{aligned} \tag{42}$$

Now, equating for $\rho = 0$ and applying T_σ to both sides of $\mathrm{Res}\upsilon_2(\vartheta,\ \rho)$ yields:

$$\omega_2(\vartheta) = \omega_0^3(\vartheta)\omega_1'''(\vartheta) + 3\omega_0^2(\vartheta)\omega_1(\vartheta)\omega_0'''(\vartheta),$$

$$\omega_2(\vartheta) = -\frac{b^3}{2\left(a - \frac{3\sqrt{b}\vartheta}{2}\right)^{4/3}}. \tag{43}$$

Consequently, the following are the second RPS approximations of the nonlinear Harry Dym equation:

$$\upsilon_2(\vartheta,\ \rho) = \omega(\vartheta) + \frac{\rho^\sigma(\omega_0^3(\vartheta)\omega_0'''(\vartheta))}{\sigma} + \frac{\rho^{2\sigma}\left(\omega_0^3(\vartheta)\omega_1'''(\vartheta) + 3\omega_0^2(\vartheta)\omega_1(\vartheta)\omega_0'''(\vartheta)\right)}{2\sigma^2},$$

$$\upsilon_2(\vartheta,\ \rho) = \left(a - \frac{3\sqrt{b}\vartheta}{2}\right)^{2/3} + \frac{\left(-\frac{b^{3/2}}{3\sqrt{a - \frac{3\sqrt{b}\vartheta}{2}}}\right)\rho^\sigma}{\sigma} + \frac{\left(-\frac{b^3}{2\left(a - \frac{3\sqrt{b}\vartheta}{2}\right)^{4/3}}\right)\rho^{2\sigma}}{2\sigma^2}. \tag{44}$$

Similarly, we use the same process for $n = 3$ to get the following outcomes:

$$\omega_3(\vartheta) = \omega_0^3(\vartheta)\omega_2'''(\vartheta) + 3\omega_0^2(\vartheta)\omega_2(\vartheta)\omega_0'''(\vartheta) + 3\omega_0^2(\vartheta)\omega_1(\vartheta)\omega_1'''(\vartheta) + 3\omega_0(\vartheta)\omega_1^2(\vartheta)\omega_0'''(\vartheta),$$

$$\omega_3(\vartheta) = -\frac{17b^{9/2}}{2\left(a - \frac{3\sqrt{b}\vartheta}{2}\right)^{7/3}}. \tag{45}$$

$$\upsilon_3(\vartheta,\ \rho) = \omega(\vartheta) + \frac{\rho^\sigma(\omega_0^3(\vartheta)\omega_0'''(\vartheta))}{\sigma} + \frac{\rho^{2\sigma}\left(\omega_0^3(\vartheta)\omega_1'''(\vartheta) + 3\omega_0^2(\vartheta)\omega_1(\vartheta)\omega_0'''(\vartheta)\right)}{2\sigma^2}$$
$$+ \frac{\left(\omega_0^3(\vartheta)\omega_2'''(\vartheta) + 3\omega_0^2(\vartheta)\omega_2(\vartheta)\omega_0'''(\vartheta) + 3\omega_0^2(\vartheta)\omega_1(\vartheta)\omega_1'''(\vartheta) + 3\omega_0(\vartheta)\omega_1^2(\vartheta)\omega_0'''(\vartheta)\right)t^{3\sigma}}{6\sigma^3},$$

$$\upsilon_3(\vartheta,\ \rho) = \left(a - \frac{3\sqrt{b}\vartheta}{2}\right)^{2/3} \tag{46}$$
$$+ \frac{\left(-\frac{b^{3/2}}{3\sqrt{a - \frac{3\sqrt{b}\vartheta}{2}}}\right)\rho^\sigma}{\sigma} + \frac{\left(-\frac{b^3}{2\left(a - \frac{3\sqrt{b}\vartheta}{2}\right)^{4/3}}\right)\rho^{2\sigma}}{2\sigma^2} + \frac{\left(-\frac{17b^{9/2}}{2\left(a - \frac{3\sqrt{b}\vartheta}{2}\right)^{7/3}}\right)\rho^{3\sigma}}{6\sigma^3}.$$

Table 1 presents a numerical comparison between the exact solution and the fourth-order approximate RPSCM solutions of the nonlinear Harry Dym equation.

$$\upsilon(\vartheta,\ \rho) = \left(a - \frac{3}{2}\sqrt{b}(\vartheta + b\rho)\right)^{2/3}. \tag{47}$$

Table 1. Analysis of various fractional order for $\rho = 0.3$ of Example 1 using RPS

ϑ	RPS$_\sigma = 0.6$	RPS$_\sigma = 0.8$	RPS$_\sigma = 1$	Exact$_\sigma = 1$	Absolute error$_\sigma = 1$
0.0	1.7487	1.79027	1.81276	1.81277	1.33831×10^{-5}
0.1	1.62677	1.67003	1.69333	1.69335	1.74536×10^{-5}
0.2	1.49999	1.54529	1.56953	1.56955	2.35036×10^{-5}
0.3	1.36741	1.41526	1.44063	1.44066	3.29591×10^{-5}
0.4	1.22771	1.27891	1.30567	1.30572	4.87203×10^{-5}
0.5	1.07878	1.13477	1.16332	1.1634	7.73366×10^{-5}
0.6	0.91691	0.980586	1.01162	1.01175	1.35843×10^{-4}
0.7	0.73379	0.812531	0.847442	0.847721	2.78489×10^{-4}
0.8	0.502197	0.622368	0.665115	0.665858	7.42739×10^{-4}
0.9	0.0405885	0.379045	0.450855	0.454264	3.40912×10^{-3}
1.0	-8.69723	-0.783118	0.0738184	0.168227	9.44085×10^{-2}

In Figure 1, the comparison of NIM solution and exact for 3D and 2D plot of $u(\vartheta,\ \rho)$ for $\rho = 0.01$ for various values of $\sigma = 1$, $\sigma = 0.8$, $\sigma = 0.6$, and $\sigma = 0.4$ of various fractional order.

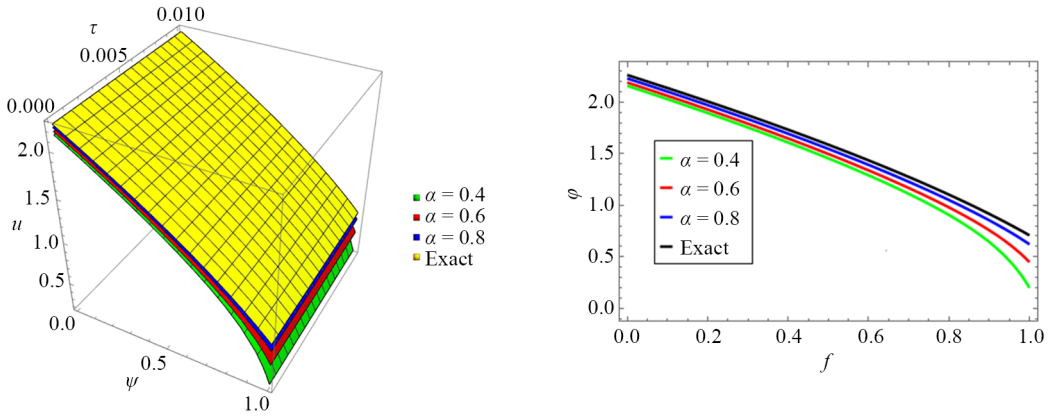

Figure 1. Comparison of NIM solution and exact for 3D and 2D plot

In Figure 2, 3D plot of RPS solution of $u(\vartheta,\ \rho)$ for $\rho = 0.01$ for various values of $\sigma = 1$, $\sigma = 0.8$, $\sigma = 0.6$, and $\sigma = 0.4$ of various fractional order.

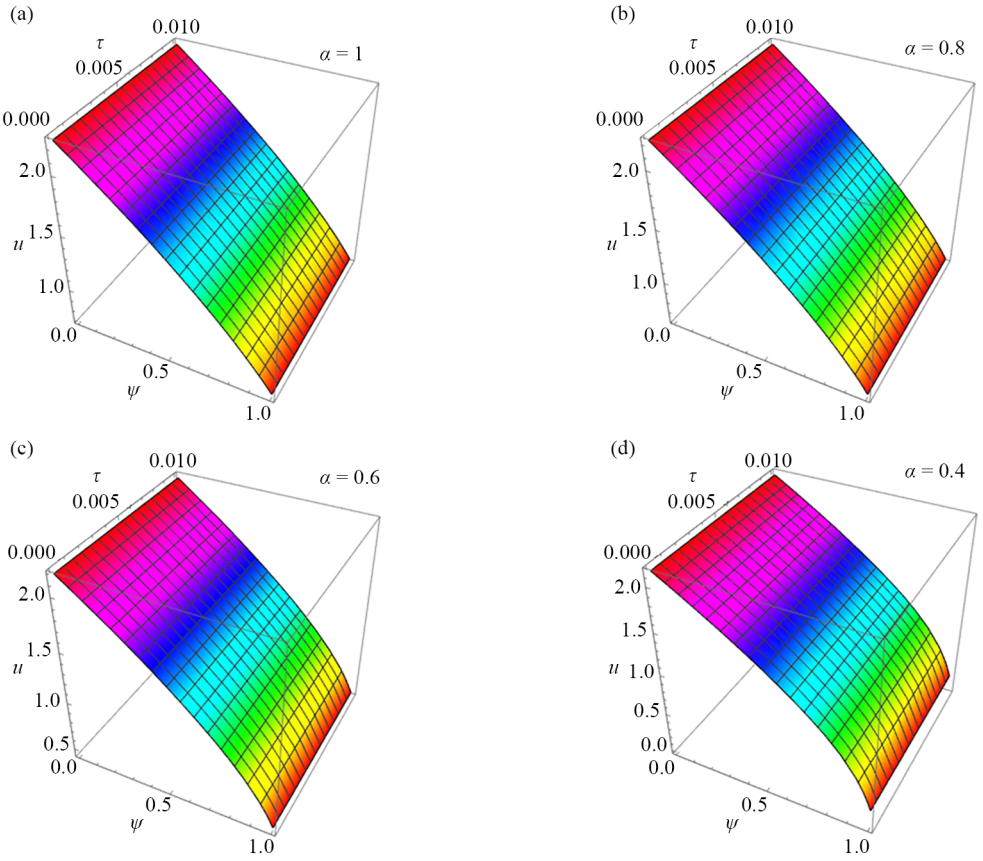

Figure 2. 3D plot of RPS solution of $u(\vartheta,\ \rho)$ for $\rho = 0.01$

5.1.1 *Implementation of NIM*

We derive the corresponding form for the conformable derivative by applying NIM procedure:

$$\frac{\partial \upsilon}{\partial \rho} = \upsilon^3(\vartheta,\ \rho)\frac{\partial^3 \upsilon(\vartheta,\ \rho)}{\partial \vartheta^3}. \tag{48}$$

using the initial condition's

$$\upsilon(\vartheta,\ 0) = \left(a - \frac{3\sqrt{b}\vartheta}{2}\right)^{2/3}. \tag{49}$$

We obtain the following several terms based on the NIM procedure:

$$\upsilon_0(\vartheta,\ \rho) = \left(a - \frac{3\sqrt{b}\vartheta}{2}\right)^{2/3},$$

$$\upsilon_1(\vartheta,\ \rho) = -\frac{b^{3/2}\rho^{\sigma}}{\sigma\sqrt[3]{a-\frac{3\sqrt{b}\vartheta}{2}}},$$

$$\upsilon_2(\vartheta,\ \rho) = -\frac{b^{3}\rho^{3\sigma}}{4\sigma^{3}\left(a-\frac{3\sqrt{b}\vartheta}{2}\right)^{4/3}}, \tag{50}$$

$$\upsilon_3(\vartheta,\ \rho) = \frac{\sqrt[3]{2}b^{9/2}\rho^{5\sigma}\left(15\sigma-16\rho^{\sigma}\right)}{3\sigma^{6}\left(2a-3\sqrt{b}\vartheta\right)^{7/3}}.$$

The final NIM algorithm solution is as follows:

$$\upsilon(\vartheta,\ \rho) = \upsilon_0(\vartheta)+\upsilon_1(\vartheta)+\upsilon_2(\vartheta)+\upsilon_3(\vartheta)+\cdots, \tag{51}$$

$$\begin{aligned}\upsilon(\vartheta,\ \rho) = &\left(a-\frac{3\sqrt{b}\vartheta}{2}\right)^{2/3}\\ &-\frac{b^{3/2}\rho^{\sigma}}{\sigma\sqrt[3]{a-\frac{3\sqrt{b}\vartheta}{2}}}-\frac{b^{3}\rho^{3\sigma}}{4\sigma^{3}\left(a-\frac{3\sqrt{b}\vartheta}{2}\right)^{4/3}}-\frac{b^{3}\rho^{3\sigma}}{4\sigma^{3}\left(a-\frac{3\sqrt{b}\vartheta}{2}\right)^{4/3}}+\frac{3\sqrt{2}b^{9/2}\rho^{5\sigma}\left(15\sigma-16\rho^{\sigma}\right)}{3\sigma^{6}\left(2a-3\sqrt{b}\vartheta\right)^{7/3}}.\end{aligned} \tag{52}$$

In Figure 3, the comparison of NIM solution and exact for 3D and 2D plot of $\upsilon(\vartheta,\ \rho)$ for $\rho = 0.01$ for various values of $\sigma = 1$, $\sigma = 0.8$, $\sigma = 0.6$, and $\sigma = 0.4$ of various fractional order.

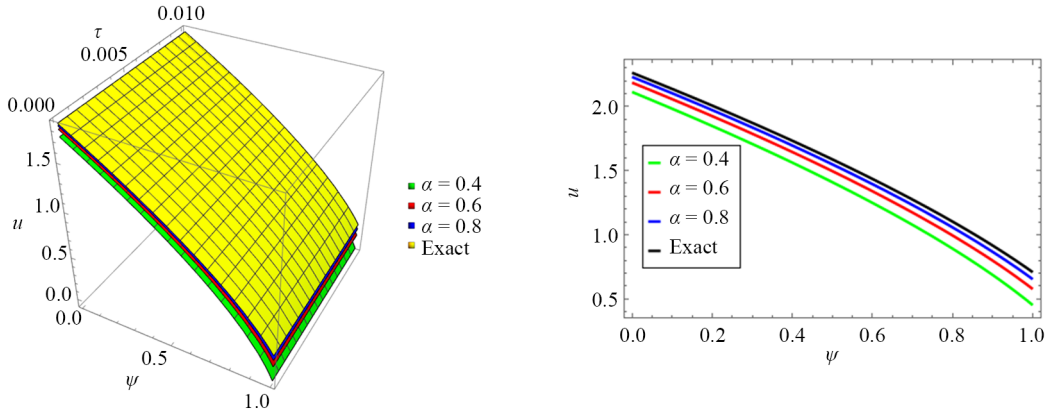

Figure 3. Comparison of NIM solution and exact for 3D and 2D plot

In Figure 4, the 3D plot of NIM solution of $\upsilon(\vartheta,\ \rho)$ for $\rho = 0.01$ for various values of $\sigma = 1$, $\sigma = 0.8$, $\sigma = 0.6$, and $\sigma = 0.4$ of various fractional order.

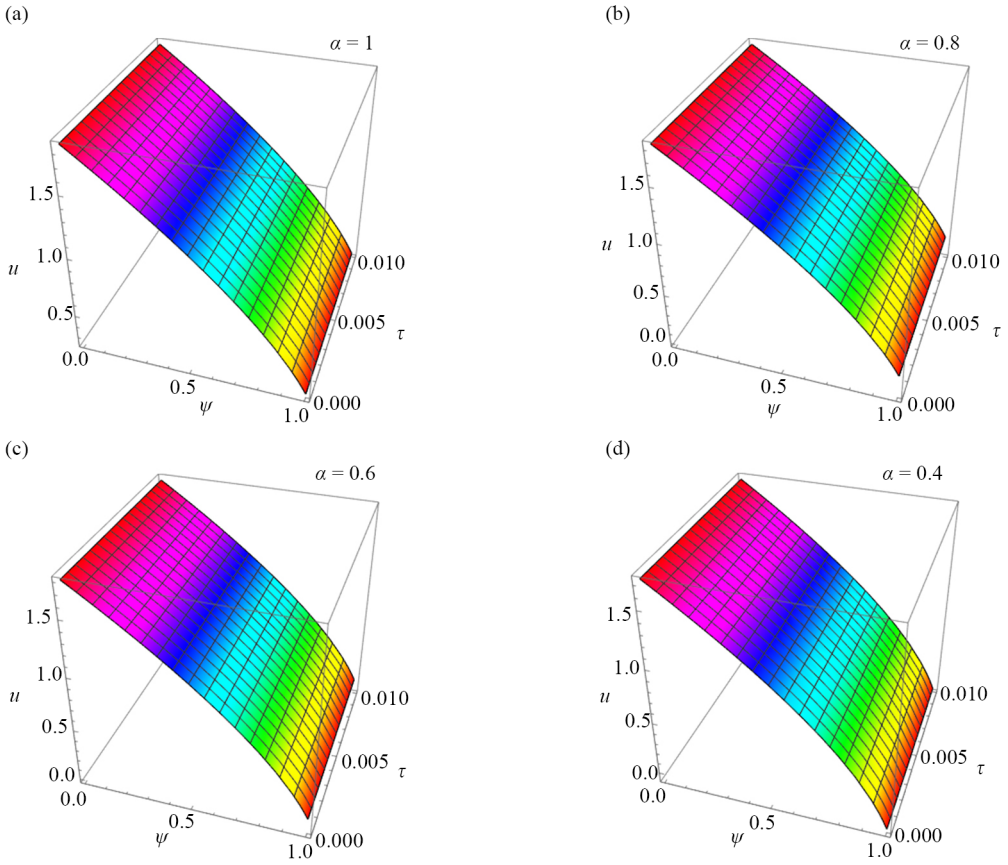

Figure 4. 3D plot of NIM solution

5.2 *Problem 2*

Let us examine the fractional-order Rosenau-Hyman Equation:

$$\frac{\partial \upsilon}{\partial \rho} - \upsilon(\vartheta,\ \rho)\frac{\partial^3 \upsilon(\vartheta,\ \rho)}{\partial \vartheta^3} - \upsilon(\vartheta,\ \rho)\frac{\partial \upsilon(\vartheta,\ \rho)}{\partial \vartheta} - 3\frac{\partial \upsilon(\vartheta,\ \rho)}{\partial \vartheta}\frac{\partial^2 \upsilon(\vartheta,\ \rho)}{\partial \vartheta^2} = 0. \tag{53}$$

using the initial condition's

$$\upsilon(\vartheta,\ 0) = \omega(\vartheta) = -\frac{8}{3}c\cos^2\left(\frac{\vartheta}{4}\right). \tag{54}$$

The exact solution for $c = 1$ is found as:

$$\upsilon(\vartheta,\ \rho) = -\frac{8}{3}c\cos^2\left(\frac{1}{4}(\vartheta - c\rho)\right). \tag{55}$$

For residual power series, where $\upsilon = \upsilon(\vartheta,\ \rho)$.

$$\upsilon(\vartheta,\ \rho) = \omega(\vartheta) + \sum_{\eta=1}^{\infty} \omega_\eta(\vartheta)\frac{\rho^{\eta\vartheta}}{\sigma^\eta \eta!} \tag{56}$$

and the truncated k-th series of $\upsilon[\vartheta,\ \rho]$.

$$\upsilon_k(\vartheta,\ \rho) = \omega(\vartheta) + \sum_{\eta=1}^{k} \omega_\eta(\vartheta)\frac{\rho^\eta}{a^\eta \eta!}, \quad k = 1,\ 2,\ 3,\ \ldots \tag{57}$$

A residual function of k-th of nonlinear Rosenau-Hyman Equation:

$$\mathrm{Re}r\,\upsilon_k(\vartheta,\ \rho) = \frac{\partial \upsilon_k}{\partial \rho} - \upsilon_k(\vartheta,\ \rho)\frac{\partial^3 \upsilon_k(\vartheta,\ \rho)}{\partial \vartheta^3} - \upsilon_k(\vartheta,\ \rho)\frac{\partial \upsilon_k(\vartheta,\ \rho)}{\partial \vartheta} - 3\frac{\partial \upsilon_k(\vartheta,\ \rho)}{\partial \vartheta}\frac{\partial^2 \upsilon_k(\vartheta,\ \rho)}{\partial \vartheta^2}. \tag{58}$$

The 1st truncated series $\upsilon_1(\vartheta,\ \rho) = \omega(\vartheta) + \omega_1(\vartheta)\dfrac{\rho^\sigma}{\sigma}$ should be substituted into the $1s\rho$ truncated residual function in order to get the coefficients $\omega_1(\vartheta)$ in $\upsilon_1(\vartheta,\ \rho)$.

$$\begin{aligned}\mathrm{Res}\upsilon_1(\vartheta,\ \rho) = \omega_1(\vartheta) &- \left(\omega(\vartheta) + \frac{\rho^\sigma \omega_1(\vartheta)}{\sigma}\right)\left(\omega'''(\vartheta) + \frac{\rho^\sigma \omega_1'''(\vartheta)}{\sigma}\right) \\ &- \left(\omega(\vartheta) + \frac{\rho^\sigma \omega_1(\vartheta)}{\sigma}\right)\left(\omega'(\vartheta) + \frac{\rho^\sigma \omega_1'(\vartheta)}{\sigma}\right) \\ &- 3\left(\omega'(\vartheta) + \frac{\rho^\sigma \omega_1'(\vartheta)}{\sigma}\right)\left(\omega''(\vartheta) + \frac{\rho^\sigma \omega_1''(\vartheta)}{\sigma}\right).\end{aligned} \tag{59}$$

Using Equation $\mathrm{Res}\upsilon_1(\vartheta,\ \rho)$, we can now substitute $\rho = 0$ and get

$$\mathrm{Resm}\upsilon_1(\vartheta,\ 0) = \omega_1(\vartheta) - \omega_0(\vartheta)\omega_0'(\vartheta) - 3\omega_0'(\vartheta)\omega_0''(\vartheta) - \omega_0(\vartheta)\omega_0'''(\vartheta). \tag{60}$$

Thus for $\mathrm{Re}\upsilon_1(\vartheta,\ 0) = 0$.

$$\omega_1(\vartheta) = \omega_0(\vartheta)\omega_0'(\vartheta) + 3\omega_0'(\vartheta)\omega_0''(\vartheta) + \omega_0(\vartheta)\omega_0'''(\vartheta). \tag{61}$$

$$\omega_1(\vartheta) = -\frac{2}{3}c^2 \sin\left(\frac{\vartheta}{2}\right). \tag{62}$$

Consequently, the first RPS approximations of the nonlinear Rosenau-Hyman Equation:

$$\upsilon_1(\vartheta,\, \rho) = \omega(\vartheta) + \frac{\omega_0(\vartheta)\omega_0'(\vartheta) + 3\omega_0'(\vartheta)\omega_0''(\vartheta) + \omega_0(\vartheta)\omega_0'''(\vartheta)}{\sigma}, \tag{63}$$

$$\upsilon_1(\vartheta,\, \rho) = -\frac{8}{3}c\cos^2\left(\frac{\vartheta}{4}\right) + \frac{\left(-\frac{2}{3}c^2 \sin\left(\frac{\vartheta}{2}\right)\right)\rho^\sigma}{\sigma}. \tag{64}$$

Once more, we use the second truncated series solution $\upsilon_2(\vartheta,\, \rho) = \omega(\vartheta) + \omega_1(\vartheta)\frac{\rho^\sigma}{\sigma} + \omega_2(\vartheta)\frac{\rho^{2\sigma}}{2\sigma^2}$ to find the second unknown coefficient $\omega_2(\vartheta)$.

$$\begin{aligned}
\mathrm{Res}\upsilon_2(\vartheta,\, \rho) = {} & \omega_1(\vartheta) + \frac{\rho^\sigma \omega_2(\vartheta)}{\sigma} \\
& - \left(\omega(\vartheta) + \frac{\rho^\sigma \omega_1(\vartheta)}{\sigma} + \omega_2(\vartheta)\frac{\rho^{2\sigma}}{2\sigma^2}\right)\left(\omega'''(\vartheta) + \frac{\rho^\sigma \omega_1'''(\vartheta)}{\sigma} + \omega_2'''(\vartheta)\frac{\rho^{2\sigma}}{2\sigma^2}\right) \\
& - \left(\omega(\vartheta) + \frac{\rho^\sigma \omega_1(\vartheta)}{\sigma} + \omega_2(\vartheta)\frac{\rho^{2\sigma}}{2\sigma^2}\right)\left(\omega'(\vartheta) + \frac{\rho^\sigma \omega_1'(\vartheta)}{\sigma} + \omega_2'(\vartheta)\frac{\rho^{2\sigma}}{2\sigma^2}\right) \\
& - 3\left(\omega'(\vartheta) + \frac{\rho^\sigma \omega_1'(\vartheta)}{\sigma} + \omega_2'(\vartheta)\frac{\rho^{2\sigma}}{2\sigma^2}\right)\left(\omega''(\vartheta) + \frac{\rho^\sigma \omega_1''(\vartheta)}{\sigma} + \omega_2''(\vartheta)\frac{\rho^{2\sigma}}{2\sigma^2}\right).
\end{aligned} \tag{65}$$

Now, equating for $\rho = 0$ and applying T_σ to both sides of $\mathrm{Res}\upsilon_2(\vartheta,\, \rho)$ yields:

$$\begin{aligned}
&\omega_2(\vartheta) = \omega_0(\vartheta)\omega_1'(\vartheta) + \omega_1(\vartheta)\omega_0'(\vartheta) + 3\omega_0'(\vartheta)\omega_1''(\vartheta) + 3\omega_1'(\vartheta)\omega_0''(\vartheta) + \omega_0(\vartheta)\omega_1'''(\vartheta) + \omega_1(\vartheta)\omega_0'''(\vartheta), \\
&\omega_2(\vartheta) = \frac{1}{3}c^3 \cos\left(\frac{\vartheta}{2}\right).
\end{aligned} \tag{66}$$

Consequently, the following are the second RPS approximations of the nonlinear Rosenau-Hyman Equation:

$$\upsilon_2(\vartheta,\,\rho)=\omega(\vartheta)+\frac{\omega_0(\vartheta)\omega_0'(\vartheta)+3\omega_0'(\vartheta)\omega_0''(\vartheta)+\omega_0(\vartheta)\omega_0'''(\vartheta)}{\sigma}$$

$$\rho^{2\sigma}(\,\omega_0(\vartheta)\,\omega_1'(\vartheta)+\omega_1(\vartheta)\,\omega_0'(\vartheta)+3\,\omega_0'(\vartheta)\,\omega_1''(\vartheta)+3\,\omega_1'(\vartheta)\,\omega_0''(\vartheta)$$

$$+\frac{+\omega_0(\vartheta)\,\omega_1'''(\vartheta)+\omega_1(\vartheta)\,\omega_0'''(\vartheta))}{2\sigma^2}, \tag{67}$$

$$\upsilon_2(\vartheta,\,\rho)=-\frac{8}{3}c\cos^2\left(\frac{\vartheta}{4}\right)+\frac{\left(-\frac{2}{3}c^2\sin\left(\frac{\vartheta}{2}\right)\right)\rho^{\sigma}}{\sigma}+\frac{\left(\frac{1}{3}c^3\cos\left(\frac{\vartheta}{2}\right)\right)\rho^{2\sigma}}{2\sigma^2}.$$

Similarly, we use the same process for $n=3$ to get the following outcomes:

$$\omega_3(\vartheta)=\omega_0(\vartheta)\omega_2'(\vartheta)+\omega_1(\vartheta)\omega_1'(\vartheta)+\omega_2(\vartheta)\omega_1'(\vartheta)+3\omega_0'(\vartheta)\omega_2''(\vartheta)+3\omega_1'(\vartheta)\omega_1''(\vartheta)+3\omega_2'(\vartheta)\omega_0''(\vartheta)$$

$$+\omega_0(\vartheta)\omega_2'''(\vartheta)+\omega_1(\vartheta)\omega_1'''(\vartheta)+\omega_2(\vartheta)\omega_0'''(\vartheta), \tag{68}$$

$$\omega_3(\vartheta)=\frac{1}{6}c^4\sin\left(\frac{\vartheta}{2}\right).$$

$$\upsilon_3(\vartheta,\,\rho)=\omega(\vartheta)+\frac{\omega_0(\vartheta)\omega_0'(\vartheta)+3\omega_0'(\vartheta)\omega_0''(\vartheta)+\omega_0(\vartheta)\omega_0'''(\vartheta)}{\sigma}$$

$$\rho^{2\sigma}(\omega_0(\vartheta)\,\omega_1'(\vartheta)+\omega_1(\vartheta)\,\omega_0'(\vartheta)+3\,\omega_0'(\vartheta)\,\omega_1''(\vartheta)+3\,\omega_1'(\vartheta)\,\omega_0''(\vartheta)$$

$$+\frac{+\omega_0(\vartheta)\,\omega_1'''(\vartheta)+\omega_1(\vartheta)\,\omega_0'''(\vartheta))}{2\sigma^2}$$

$$(\omega_0(\vartheta)\,\omega_2'(\vartheta)+\omega_1(\vartheta)\,\omega_1'(\vartheta)+\omega_2(\vartheta)\,\omega_1'(\vartheta)+3\,\omega_0'(\vartheta)\,\omega_2''(\vartheta)+3\,\omega_1'(\vartheta)\,\omega_1''(\vartheta)$$

$$+\frac{+3\,\omega_2'(\vartheta)\,\omega_0''(\vartheta)+\omega_0(\vartheta)\,\omega_2'''(\vartheta)+\omega_1(\vartheta)\,\omega_1'''(\vartheta)+\omega_2(\vartheta)\,\omega_0'''(\vartheta))\rho^{3\sigma}}{6\sigma^3} \tag{69}$$

$$\upsilon_3(\vartheta,\,\rho)=-\frac{8}{3}c\cos^2\left(\frac{\vartheta}{4}\right)+\frac{\left(-\frac{2}{3}c^2\sin\left(\frac{\vartheta}{2}\right)\right)\rho^{\sigma}}{\sigma}+\frac{\left(\frac{1}{3}c^3\cos\left(\frac{\vartheta}{2}\right)\right)\rho^{2\sigma}}{2\sigma^2}+\frac{\left(\frac{1}{6}c^4\sin\left(\frac{\vartheta}{2}\right)\right)\rho^{3\sigma}}{6\sigma^3}.$$

Table 1 presents a numerical comparison between the exact solution and the fourth-order approximate RPSCM solutions of the nonlinear Rosenau-Hyman Equation.

$$\upsilon(\vartheta,\,\rho)=-\frac{8}{3}c\cos^2\left(\frac{1}{4}(\vartheta-c\rho)\right). \tag{70}$$

In Figure 5, the comparison of 3D and 2D plot of $\upsilon(\vartheta,\ \rho)$ for $\rho = 1$ and $c = 1$for various values of $\sigma = 1$, $\sigma = 0.8$, $\sigma = 0.6$, and $\sigma = 0.4$ of various fractional order.

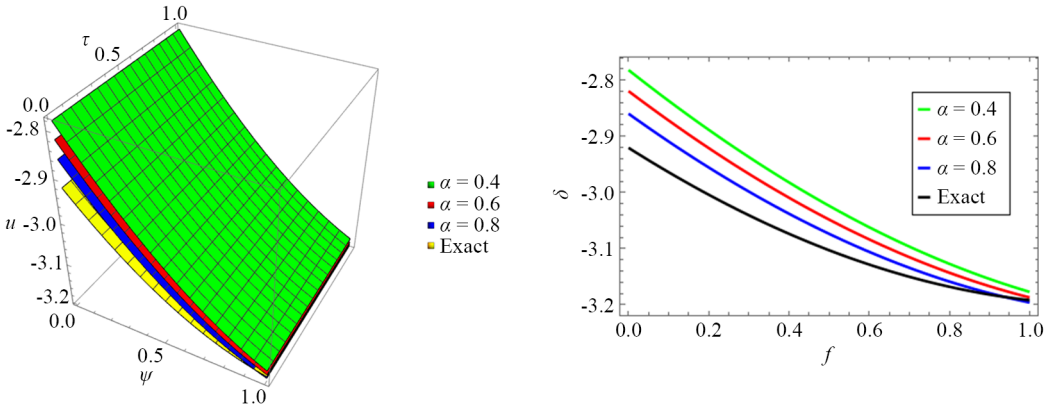

Figure 5. Comparison of 3D and 2D plot

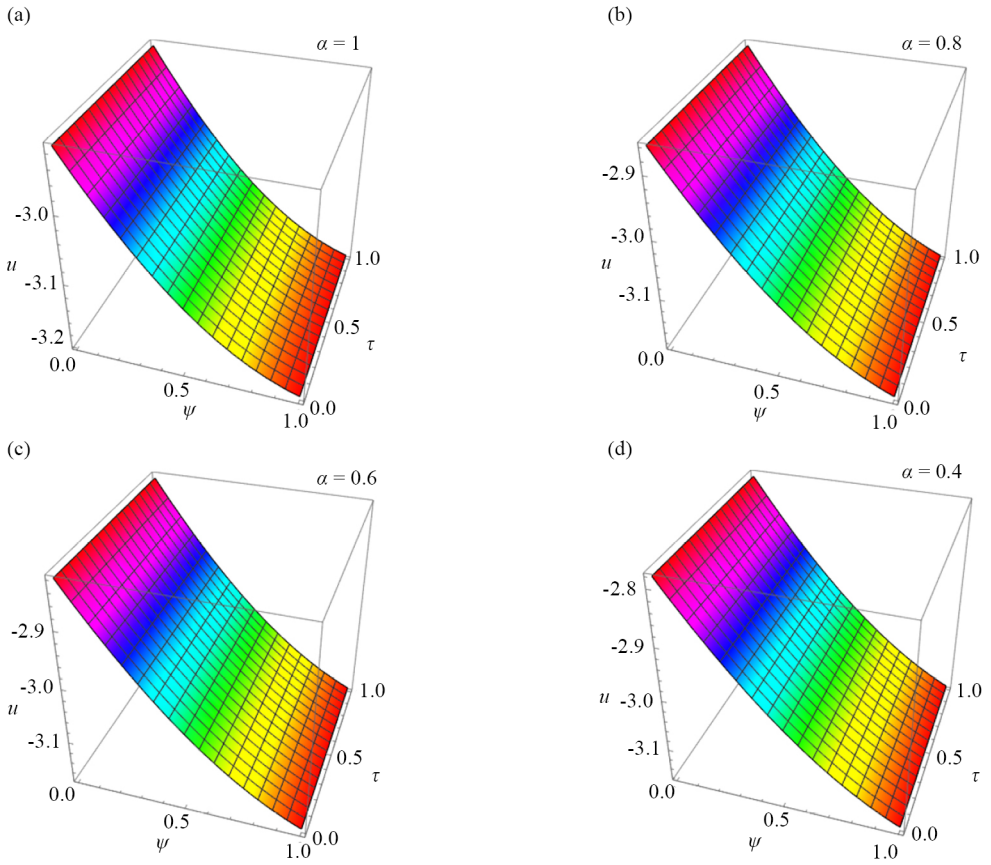

Figure 6. In figure 6, 3D plot of RPS solution of $\upsilon(\vartheta,\ \rho)$ for $\rho = 1$ and $c = 1$ for various values of $\sigma = 1$, $\sigma = 0.8$, $\sigma = 0.6$, and $\sigma = 0.4$ of various fractional order

5.2.1 *Implementation of NIM*

We derive the corresponding form for the conformable derivative by applying NIM procedure:

$$\frac{\partial \upsilon}{\partial \rho} = \upsilon(\vartheta,\ \rho)\frac{\partial^3 \upsilon(\vartheta,\ \rho)}{\partial \vartheta^3} + \upsilon(\vartheta,\ \rho)\frac{\partial \upsilon(\vartheta,\ \rho)}{\partial \vartheta} + 3\frac{\partial \upsilon(\vartheta,\ \rho)}{\partial \vartheta}\frac{\partial^2 \upsilon(\vartheta,\ \rho)}{\partial \vartheta^2}. \tag{71}$$

With the following initial conditions:

$$\upsilon(\vartheta,\ 0) = -\frac{8}{3}c\cos^2\left(\frac{\vartheta}{4}\right). \tag{72}$$

We obtain the following several terms based on the NIM procedure:

$$\begin{aligned}
\upsilon_0 &= -\frac{8}{3}c\cos^2\left(\frac{\vartheta}{4}\right),\\
\upsilon_1(\vartheta,\ \rho) &= -\frac{2c^2\rho^{\sigma}\sin\left(\frac{\vartheta}{2}\right)}{3\sigma},\\
\upsilon_2(\vartheta,\ \rho) &= \frac{c^3\rho^{3\sigma}\cos\left(\frac{\vartheta}{2}\right)}{6\sigma^2},\\
\upsilon_3(\vartheta,\ \rho) &= \frac{c^4\rho^{6\sigma}\sin\left(\frac{\vartheta}{2}\right)}{72\sigma^5}.
\end{aligned} \tag{73}$$

The final NIM algorithm solution is as follows:

$$\upsilon(\vartheta,\ \rho) = \upsilon_0(\vartheta) + \upsilon_1(\vartheta) + \upsilon_2(\vartheta) + \upsilon_3(\vartheta) + \cdots, \tag{74}$$

$$\upsilon(\vartheta,\ \rho) = -\frac{8}{3}c\cos^2\left(\frac{\vartheta}{4}\right) - \frac{2c^2\rho^{\sigma}\sin\left(\frac{\vartheta}{2}\right)}{3\sigma} + \frac{c^3\rho^{3\sigma}\cos\left(\frac{\vartheta}{2}\right)}{6\sigma^2} + \frac{c^4\rho^{6\sigma}\sin\left(\frac{\vartheta}{2}\right)}{72\sigma^5}. \tag{75}$$

6. Graphical and tables discussion

In this study, we evaluated the effectiveness of the Residual Power Series Conformable Method (RPSCM) and a Novel Iterative Method (NIM) for solving the fractional nonlinear Harry-Dym and Rosenau-Hyman equations using conformable fractional derivatives. The comparison of these methods, presented through various figures and tables, highlights their accuracy and computational efficiency in obtaining approximate solutions for these challenging equations. Table 1 shows the analysis of various fractional orders for $\rho = 0.3$ of Example 1 using RPS. This table demonstrates how the solution

behavior of $\upsilon(\vartheta,\ \rho)$ varies as the fractional order changes, revealing the sensitivity of the solution to the fractional derivative. Figure 1 presents a comparison between the NIM solution and the exact solution for both 3D and 2D plots of $\upsilon(\vartheta,\ \rho)$ for $\rho = 0.01$. It includes results for various values of $\sigma = 1$, $\sigma = 0.8$, $\sigma = 0.6$, and $\sigma = 0.4$, for different fractional orders. The plots clearly show how the solution behaves for different fractional orders, offering insights into the convergence and accuracy of the NIM. Figure 2 illustrates the 3D plot of the RPS solution for $\upsilon(\vartheta,\ \rho)$ at $\rho = 0.01$, again for varying values of σ and fractional orders. This figure allows a detailed view of how the solution changes with fractional order and highlights the RPS method's effectiveness in capturing the dynamics of the system. Table 2 provides a similar analysis for the NIM method, presenting the fractional order analysis for $\rho = 0.3$ of Example 1. It serves as a comparison to Table 1, emphasizing the differences in the solutions obtained from the two methods. Figure 3 presents the comparison of the NIM solution and the exact solution for both 3D and 2D plots of $\upsilon(\vartheta,\ \rho)$ for $\rho = 0.01$. The plots, like those in Figure 1, help visualize the performance of the NIM for various fractional orders and show the differences in solution accuracy for different values of σ. Figure 4 shows the 3D plot of the NIM solution for $\upsilon(\vartheta,\ \rho)$ at $\rho = 0.01$, again for varying fractional orders. This figure demonstrates how the NIM method captures the solution dynamics across different fractional orders and provides a clear view of the solution's sensitivity to these variations. Table 3 displays the analysis of fractional orders for $\rho = 0.5$ and $c = 1$ of Example 2 using RPS. This table provides an additional test case, further highlighting the robustness of the RPS method in handling different problem settings. It shows the impact of fractional order on the solution $\upsilon(\vartheta,\ \rho)$ for varying values of σ. Figure 5 compares the 3D and 2D plots of $\upsilon(\vartheta,\ \rho)$ for $\rho = 1$ and $c = 1$, for varying values of σ and fractional orders. The comparison of the RPS solution with the exact solution provides an assessment of the accuracy and convergence of the RPS method for this case. Figure 6 shows the 3D plot of the RPS solution for $\upsilon(\vartheta,\ \rho)$ at $\rho = 1$ and $c = 1$, for different fractional orders. This figure illustrates how the solution evolves as fractional order changes, highlighting the influence of σ and fractional order on the behavior of the system. Table 4 presents the analysis of various fractional orders for $\rho = 0.5$ and $c = 1$ of Example 1 using NIM. This provides a direct comparison with Table 3, highlighting the differences in solution accuracy and convergence when using the two methods. Figure 7 shows the comparison of the NIM solution with the exact solution for both 3D and 2D plots of $\upsilon(\vartheta,\ \rho)$ at $\rho = 1$ and $c = 1$. It clearly demonstrates the differences in the solutions for various fractional orders, giving insights into the convergence and accuracy of the NIM. Figure 8 presents the 3D plot of the NIM solution for $\upsilon(\vartheta,\ \rho)$ at $\rho = 1$ and $c = 1$, for varying fractional orders. This figure further emphasizes the behavior of the solution for different fractional orders and values of σ, showcasing how the NIM adapts to these changes.

Table 2. Analysis of various fractional order for $\rho = 0.3$ of Example 1 using NIM

ϑ	NIM$_{\sigma} = 0.6$	NIM$_{\sigma} = 0.8$	NIM$_{\sigma} = 1$	Exact$_{\sigma} = 1$	Absolute error$_{\sigma} = 1$
0.0	1.53451	1.75053	1.81289	1.81277	1.15206×10^{-4}
0.1	1.40557	1.62901	1.69348	1.69335	1.31731×10^{-4}
0.2	1.27082	1.50281	1.56971	1.56955	1.52902×10^{-4}
0.3	1.12909	1.37111	1.44084	1.44066	1.8084×10^{-4}
0.4	0.978794	1.23281	1.30594	1.30572	2.19124×10^{-4}
0.5	0.817572	1.08637	1.16367	1.1634	2.74254×10^{-4}
0.6	0.64177	0.929489	1.01211	1.01175	3.59265×10^{-4}
0.7	0.445117	0.758427	0.848225	0.847721	5.04231×10^{-4}
0.8	0.215243	0.56629	0.666653	0.665858	7.95371×10^{-4}
0.9	-0.0786102	0.337131	0.455863	0.454264	1.59936×10^{-3}
1.0	-0.540982	0.00668695	0.175936	0.168227	7.70871×10^{-3}

Table 3. Analysis of various fractional order for $\rho = 0.5$ and $c = 1$ of Example 2 using RPS

ϑ	RPS$_\sigma = 0.6$	RPS$_\sigma = 0.8$	RPS$_\sigma = 1$	Exact$_\sigma = 1$	Absolute error$_\sigma = 1$
0.0	-1.32968	-1.33252	-1.33313	-1.33313	1.08504×10^{-8}
0.1	-1.33234	-1.33333	-1.33313	-1.33313	7.37605×10^{-8}
0.2	-1.33333	-1.33249	-1.33146	-1.33146	1.58187×10^{-7}
0.3	-1.33266	-1.32997	-1.32813	-1.32813	2.42218×10^{-7}
0.4	-1.33033	-1.3258	-1.32315	-1.32315	3.25644×10^{-7}
0.5	-1.32633	-1.31998	-1.31653	-1.31653	4.08256×10^{-7}
0.6	-1.32069	-1.31253	-1.30828	-1.30828	4.89847×10^{-7}
0.7	-1.31341	-1.30347	-1.29843	-1.29843	5.70214×10^{-7}
0.8	-1.30451	-1.29281	-1.28701	-1.28701	6.49156×10^{-7}
0.9	-1.29402	-1.28059	-1.27403	-1.27403	7.26475×10^{-7}
1.0	-1.28196	-1.26683	-1.25953	-1.25953	8.01979×10^{-7}

Table 4. Analysis of various fractional order for $\rho = 0.5$ and $c = 1$ of Example 1 using NIM

ϑ	NIM$_\sigma = 0.6$	NIM$_\sigma = 0.8$	NIM$_\sigma = 1$	Exact$_\sigma = 1$	Absolute error$_\sigma = 1$
0.0	-1.33332	-1.33333	-1.33333	-1.33333	2.06249×10^{-6}
0.1	-1.33336	-1.33276	-1.33258	-1.33258	2.06000×10^{-6}
0.2	-1.33174	-1.33052	-1.33017	-1.33017	2.05236×10^{-6}
0.3	-1.32845	-1.32663	-1.3261	-1.32609	2.03959×10^{-6}
0.4	-1.32351	-1.32108	-1.32038	-1.32037	2.02173×10^{-6}
0.5	-1.31693	-1.3139	-1.31302	-1.31302	1.99881×10^{-6}
0.6	-1.30872	-1.3051	-1.30405	-1.30405	1.97089×10^{-6}
0.7	-1.29891	-1.29471	-1.29349	-1.29348	1.93805×10^{-6}
0.8	-1.28752	-1.28274	-1.28136	-1.28135	1.90036×10^{-6}
0.9	-1.27458	-1.26924	-1.26769	-1.26769	1.85792×10^{-6}
1.0	-1.26011	-1.25423	-1.25252	-1.25252	1.81084×10^{-6}

In Figure 7, the comparison of 3D and 2D plot with exact solution of $u(\vartheta,\ \rho)$ for $\rho = 1$ and $c = 1$ for various values of $\sigma = 1$, $\sigma = 0.8$, $\sigma = 0.6$, and $\sigma = 0.4$ of various fractional order.

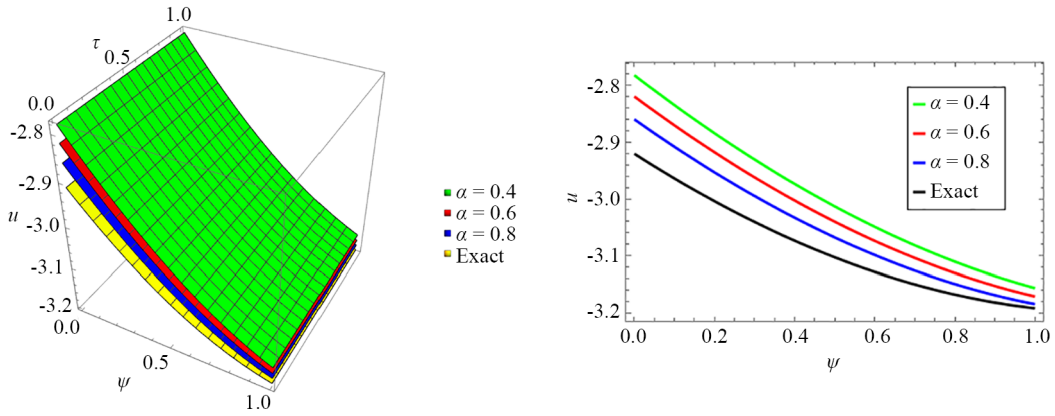

Figure 7. Comparison of 3D and 2D plot

In Figure 8, the 3D plot of NIM solution of $u(\vartheta,\ \rho)$ for $\rho = 1$ and $c = 1$ for various values of $\sigma = 1$, $\sigma = 0.8$, $\sigma = 0.6$, and $\sigma = 0.4$ of various fractional order.

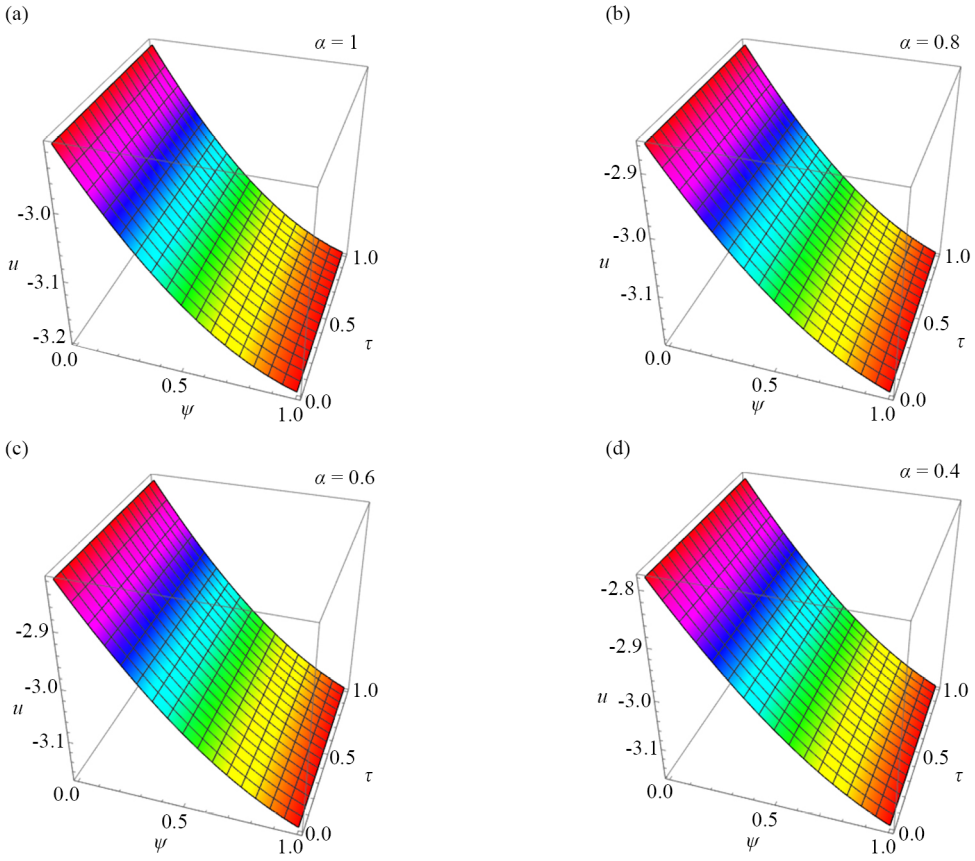

Figure 8. 3D plot of NIM solution

Overall, the graphical results provide a comprehensive view of how both the RPSCM and NIM methods perform in solving fractional nonlinear equations. The figures and tables validate the effectiveness of these methods, showing that both converge quickly and yield precise results. The comparison between the methods demonstrates their versatility and robustness in solving complex fractional-order equations, making them valuable tools for researchers and engineers working on fractional differential equations. Future studies can extend these methods to more complex models and explore their applications in various fields, further enhancing our understanding of non-local phenomena and their real-world applications.

7. Conclusion

In conclusion, the application of the Residual Power Series Conformable Method (RPSCM) and the novel iterative method proves to be highly effective in solving the fractional nonlinear Harry-Dym and Rosenau-Hyman equations with conformable fractional derivatives. Both methods demonstrate excellent accuracy and computational efficiency in obtaining approximate solutions to these complex equations, which are otherwise challenging to solve using traditional approaches. The results, validated through numerical simulations, show that the proposed methods converge rapidly and provide precise solutions, even for higher fractional orders. The comparison of the methods further highlights

their robustness and versatility in tackling nonlinear fractional problems. These findings suggest that the RPSCM and the iterative method offer valuable tools for researchers and engineers working on fractional differential equations in various scientific and engineering applications. Future research can extend these methods to more complex fractional models, providing deeper insights into non-local phenomena in a variety of fields.

Acknowledgements

The author is thankful to the Deanship of Graduate Studies and Scientific Research at the University of Bisha for supporting this work through the Fast-Track Research Support Program.

Conflict of interest

The authors declare no conflict of interest.

References

[1] Alharbi MH, Abu Sunayh AF, Atta AG, Abd-Elhameed WM. Novel approach by shifted fibonacci polynomials for solving the fractional Burgers equation. *Fractal and Fractional*. 2024; 8(7): 427.

[2] Youssri YH, Ismail MI, Atta AG. Chebyshev Petrov-Galerkin procedure for the time-fractional heat equation with nonlocal conditions. *Physica Scripta*. 2023; 99(1): 015251.

[3] Abd-Elhameed WM, Youssri YH, Atta AG. Tau algorithm for fractional delay differential equations utilizing seventh-kind Chebyshev polynomials. *Journal of Mathematical Modeling*. 2024; 12(2): 277-299.

[4] Chhibber PK, Majumdar SK. Foreign ownership and profitability: Property rights, control, and the performance of firms in Indian industry. *Journal of Law & Economics*. 1999; 42(1): 209-238.

[5] Caputo M, Fabrizio M. A new definition of fractional derivative without singular Kernel. *Progress in Fractional Differentiation and Applications*. 2015; 1(2): 73-85.

[6] Kilbas AA, Srivastava HM, Trujillo JJ. *Theory and Applications of Fractional Differential Equations*. Amsterdam: Elsevier; 2006.

[7] Owolabi KM, Atangana A. Chaotic behaviour in system of noninteger-order ordinary differential equations. *Chaos, Solitons and Fractals*. 2018; 115: 362-370.

[8] Kruskal MD, Moser J. *Dynamical Systems, Theory and Applications*. Berlin, Heidelberg: Springer-Verlag; 1975.

[9] Vasconcelos GL, Kadanoff LP. Stationary solutions for the Saffman-Taylor problem with surface tension. *Physical Review A*. 1991; 44(10): 6490.

[10] Gesztesy F, Unterkofler K. Isospectral deformations for Sturm-Liouville and Dirac-Type operators and associated nonlinear evolution equations. *Reports on Mathematical Physics*. 1992; 31(2): 113-137.

[11] Rosenau P, Hyman JM. Compactons: Solitons with finite wavelength. *Physical Review Letters*. 1993; 70(5): 564.

[12] Mihaila B, Cardenas A, Cooper F, Saxena A. Stability and dynamical properties of Rosenau-Hyman compactons using Padé approximants. *Physical Review E*. 2010; 81(5): 056708.

[13] Bazeia D, Das A, Losano L, Santos MJD. Traveling wave solutions of nonlinear partial differential equations. *Applied Mathematics Letters*. 2010; 23(6): 681-686.

[14] Rus F, Villatoro FR. Self-similar radiation from numerical Rosenau-Hyman compactons. *Journal of Computational Physics*. 2007; 227(1): 440-457.

[15] Rus F, Villatoro FR. Padé numerical method for the Rosenau-Hyman compacton equation. *Mathematics and Computers in Simulation*. 2007; 76(1-3): 188-192.

[16] Akram T, Abbas M, Riaz MB, Ismail AI, Ali NM. An efficient numerical technique for solving time fractional Burgers equation. *Alexandria Engineering Journal*. 2020; 59(4): 2201-2220.

[17] Al-Smadi M. Fractional residual series for conformable time fractional Sawada-Kotera-Ito, Lax, and Kaup-Kupershmidt equations of seventh order. *Mathematical Methods in the Applied Sciences*. 2021; 44(1): 1-21.

[18] Khalid N, Abbas M, Iqbal MK, Baleanu D. A numerical investigation of Caputo time fractional Allen-Cahn equation using redefined cubic B-spline functions. *Advances in Difference Equations*. 2020; 2020(1): 158.
[19] Khalid N, Abbas M, Iqbal MK, Singh J, Ismail AIM. A computational approach for solving time fractional differential equation via spline functions. *Alexandria Engineering Journal*. 2020; 59(5): 3061-3078.
[20] Bira B, Raja Sekhar T, Zeidan D. Exact solutions for some time-fractional evolution equations using Lie group theory. *Mathematical Methods in the Applied Sciences*. 2018; 41(16): 6717-6725.
[21] Daftardar-Gejji V, Jafari H. An iterative method for solving nonlinear functional equations. *Journal of Mathematical Analysis and Applications*. 2006; 316(2): 753-763.
[22] He JH. Homotopy perturbation technique. *Computer Methods in Applied Mechanics and Engineering*. 1999; 178(3-4): 257-262.
[23] Adomian G. *Solving Frontier Problems of Physics: The Decomposition Method*. Dordrecht: Springer Science & Business Media; 2013.
[24] He JH. Approximate analytical solution for seepage flow with fractional derivatives in porous media. *Computer Methods in Applied Mechanics and Engineering*. 1998; 167(1-2): 57-68.
[25] Daftardar-Gejji V, Bhalekar S. Solving fractional diffusion-wave equations using a new iterative method. *Fractional Calculus and Applied Analysis*. 2008; 11(2): 193-202.
[26] Das S. *Functional Fractional Calculus*. Berlin: Springer; 2011.
[27] Caputo M. Linear models of dissipation whose *Q* is almost frequency independent-II. *Geophysical Journal International*. 1967; 13(5): 529-539.
[28] Khalil R, Al Horani M, Yousef A, Sababheh M. A new definition of fractional derivative. *Journal of Computational and Applied Mathematics*. 2014; 264: 65-70.
[29] Atangana A, Baleanu D, Alsaedi A. New properties of conformable derivative. *Open Mathematics*. 2015; 13(1): 889-898.
[30] Tasbozan O, Cenesiz Y, Kurt A. New solutions for conformable fractional Boussinesq and combined KdV-mKdV equations using Jacobi elliptic function expansion method. *The European Physical Journal Plus*. 2016; 131: 1-14.
[31] El-Ajou A, Arqub OA, Zhour ZA, Momani S. New results on fractional power series: Theories and applications. *Entropy*. 2013; 15(12): 5305-5323.
[32] Abdeljawad T. On conformable fractional calculus. *Journal of Computational and Applied Mathematics*. 2015; 279: 57-66.
[33] Alquran M. Analytical solutions of fractional foam drainage equation by residual power series method. *Mathematical Sciences*. 2014; 8(4): 153-160.
[34] Jaradat HM, Al-Shara S, Khan QJ, Alquran M, Al-Khaled K. Analytical solution of time-fractional Drinfeld-Sokolov-Wilson system using residual power series method. *IAENG International Journal of Applied Mathematics*. 2016; 46(1): 64-70.
[35] Kumar A, Kumar S, Singh M. Residual power series method for fractional Sharma-Tasso-Olever equation. *Communications in Numerical Analysis*. 2016; 2016(1): 1-10.
[36] Senol M, Alquran M, Kasmaei HD. On the comparison of perturbation-iteration algorithm and residual power series method to solve fractional Zakharov-Kuznetsov equation. *Results in Physics*. 2018; 9: 321-327.